Structure maps for MAX phases formability revisited

Yiming Zhang<sup>a,\*</sup>, Yongjia Xu<sup>a</sup>, Qing Huang<sup>a</sup>, Shiyu Du<sup>a</sup>, Mian Li<sup>a</sup>, Youbing Li<sup>a</sup>, Zeyu

Mao<sup>b</sup>, Qi Han<sup>c</sup>

<sup>a</sup> Engineering Laboratory of Advanced Energy Materials, Qianwan Institute of CNiTECH,

Ningbo, China

<sup>b</sup> State Key Laboratory for Mechanical Behavior of Materials, Xi'an Jiaotong University,

Xi'an, China

<sup>c</sup> College of Science and Technology, Ningbo University, Ningbo, China

Abstract

The extraordinary chemical diversity of MAX phases raises the question of how

many and which novel ones are yet to be discovered. The conventional schemes rely

either on executions of well designed experiments or elaborately crafted calculations;

both of which have been key tactics within the past several decades that have yielded

many of important new materials we are studying and using today. However, these

approaches are expensive despite the emergence of high throughput automations or

evolution of high-speed computers. In this work, we have revisited the in prior proposed

"light-duty" strategy, i.e. structure mapping, for describing the genomic conditions under

which one MAX phase could form; that allow us to make successful formability/non-

formability separation of MAX phases with a fidelity of 95.5%. Our results suggest that

the proposed coordinates, and further the developed structure maps, are able to offer a

useful initial guiding principles for systematic screenings of potential MAX phases and

provide untapped opportunities for their structure prediction and materials design.

\* Corresponding author

E-mail address: ymzhang@nimte.ac.cn (Y. Zhang)

1

### 1. Introduction

The MAX phases, or  $M_{n+1}AX_n$ , are a family of layered compounds within the class of complex carbides, nitrides, or borides; where "M" refers to an early transition metal, "A" belongs to an A-group element, "X" can be C, N and/or B, and "n" is an integer (commonly 1, 2, or 3) [1-5]. Based on the values of integer n, the MAX phases can be subcategorized into 211, 312 and 413 structures, respectively. Fig. 1(a) illustrates the hexagonal unit cells of 211, 312 and 413 MAX phases, which consist of M<sub>6</sub>X octahedra interleaved with layers of A elements. Currently, this kind of material is keeping attractive due to: 1) their owning of unexpected combination of both metallic and ceramic properties, 2) the ease by which one can regulate their chemistry, while keeping the structures same, 3) the discovery of both in- and out-of-plane ordered phases that opens the door to broad their family members, and 4) the ease by which they can be exfoliated into their 2D counterparts, MXenes, which exhibit fascinating properties and possess high application potentials to address some of society's most pressing issues [6]. At the moment, there are around 110 ternary MAX phases been experimentally reported, and new compounds with possible M, A and X elements are still being discovered [7-17]. Further, this number increases considerably when sold solutions or medium-/high-entropy candidates are taken into accounts [7, 18-22] (shown in Fig. 1(b)). The combinatorial design space suggests that the currently known MAX phases are only the tip of the iceberg, and substantial number of hitherto-unknown candidates are awaiting to be explored. During the past decade, ab initio calculations have been extensively conducted; either through estimating whether a compound is stable on an absolute scale, or demonstrating that a given MAX phase is more stable than all other competing phases, to investigate the potential MAX phases [23-34]. The predictive power and accuracy of these tools are evident; yet without time-consuming full DFT calculations, these analyses incapable of revealing any

correlations or systematic behaviors [2, 23]. Accordingly, the extraordinary chemical diversity of MAX phases raises the issue of proposing general chemical design rules to tackle the factorial complexity of MAX phases design without arduous number crunching.

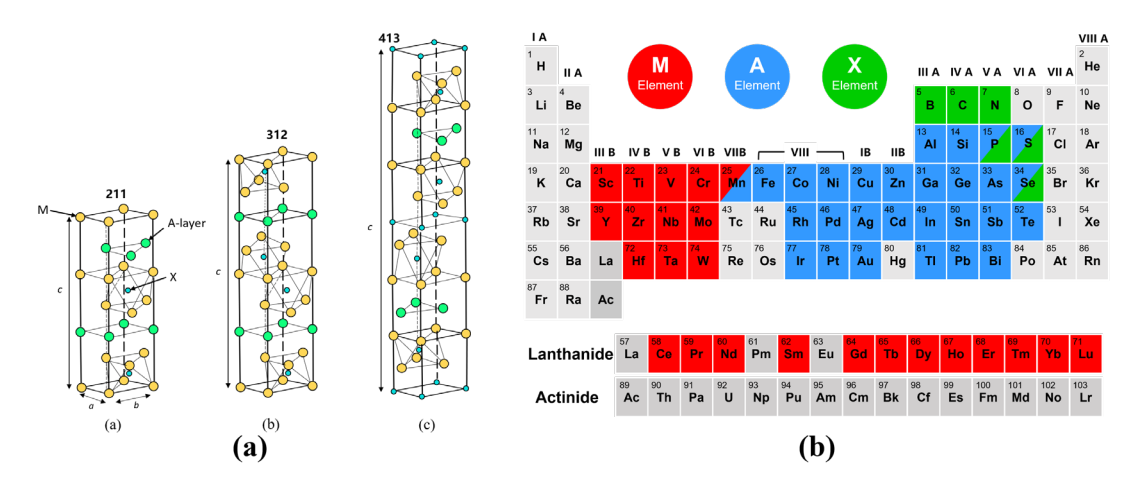


Fig. 1 (a) Crystal structures for the 211, 312 and 413 MAX phases; (b) The introduced elements within various MAX phases.

Structure mapping, a scheme tries to discern key parameters that are strongly associated with the occurrence of a given crystal chemistry, has played an important role as a useful *a priori* guide for mapping out certain crystal types and served as a visualization tool for composition-structure relationships in a bivariate way [35-42]. There is a time-honored and distinguished tradition of such maps for novel materials developments [43-58]; and currently, it has been acknowledged that this creative and insightful graphical representations of data could leverage ones to grasp most important points without laborious analysis [59, 60]. In 2020, this strategy has been implemented to develop a classification scheme for MAX phases formability/non-formability separation [6]. Currently, the buzzing characteristic of novel composition development has enriched the family members of MAX phases; and the proposed structure map need to be validated and updated against the whole members of currently known MAX phases. In this work we endeavor to propose the revisited genomic conditions, that is composing of *geometric* and *electron concentration* factors, for deriving upgraded structure maps to identify the

stability region that the  $M_{n+1}AX_n$  phases could form, which can be further adopted to guide the exploration of potential MAX phases.

# 2. Revisiting the factors regulating MAX phases

In previous work [6], the important roles of *geometrical* and *electron concentration* factors play within the formability of MAX phases are fully discussed; and the expressions of these two factors are derived accordingly (shown in Eqns. (1) and (2)).

Geometrical Factor: 
$$\frac{|R_M - R_A|}{R_M}$$
 (1)

Where  $R_M$  and  $R_A$  represent atomic radii of M-site elements and A-site elements respectively, whose values are taken from CRC Handbook [61].

Electron Concentration Factor: 
$$\frac{(VEC)_M * n_M + \left(\frac{e}{a}\right)_A * n_A + (VEC)_X * n_X}{n_M + n_A + n_X}$$
(2)

Where  $(VEC)_M$  represents the number of valence electrons of M-site elements;  $\left(\frac{e}{a}\right)_A$  represents the number of itinerant electrons of A-site elements;  $(VEC)_X$  represents the number of valence electrons of X-site elements; and  $n_M$ ,  $n_A$ ,  $n_X$  represent atomic coefficients of M-, A- and X- site elements respectively. Here, it worth noting that, although both play crucial roles for the chemical bonding, the e/a is introduced mainly for metallic bonding; whereas the VEC is defined locally for strong chemical bonding. Due to the difference, VEC takes the d-electrons accommodated in the valence band into account [62-65]. The values of valence electrons are collected from general inorganic chemistry textbook [66]; and the itinerant electrons are taken from Mizutani and Sato [63] (Table 1 lists the valence/itinerant electron values adopted in this work).

It can be noticed that the *electron concentration factor* in that study surveys the influences from M-, A- and X- site elements, as well as the stoichiometry factor, n; and the results have shown its feasibility. Therefrom the *electron concentration factor* is

inherited into current research. In contrast, for the *geometrical* factor, only the size difference between M-site and A-site elements are under consideration; where the X-site elements dimension, as well as different *n* values, is disregarded. Owing to this, the following section is devoted to revisiting the *geometrical factor* extensively.

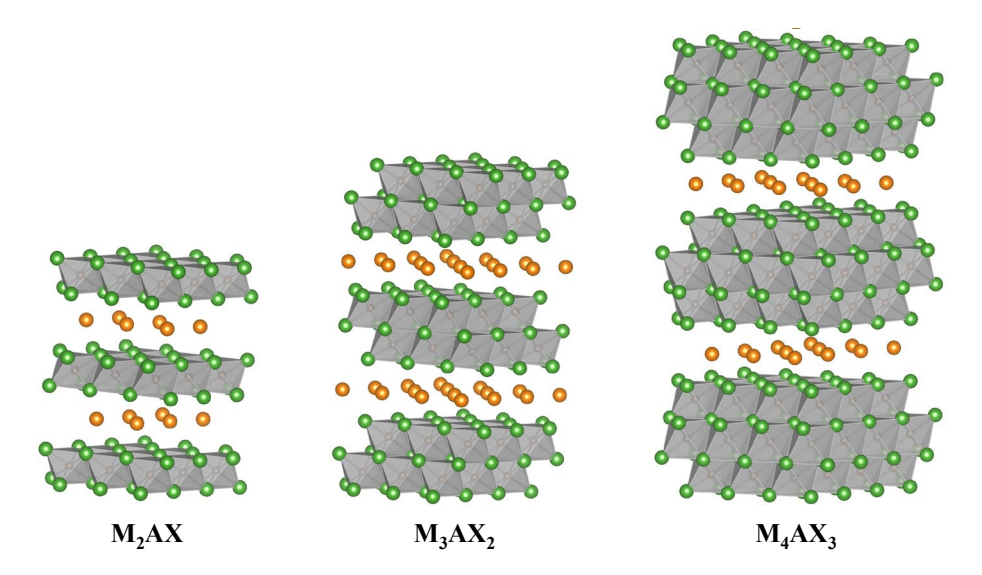


Fig. 2 Schematic illustration of the 211, 312, and 413 MAX phases crystal structure.

# 2.1 Development of intercalation factor

As one type of Nowotny octahedral phases, 211-MAX phases possess the crystal structure in which the M<sub>6</sub>X-octahedra share common edges, with A-site elements intercalated [3, 67]. Fig. 2 depicts the crystal structures of 211, 312, and 413 MAX phases, where the difference between these three structures is in the numbers of octahedra block layers. By borrowing the idea of employing the size difference to characterize the geometrical mismatch [6, 68-70], the difference between the heights of M<sub>6</sub>X octahedra/octahedron and atomic radius of A-site elements (*i.e.*, the distance between opposite faces) is adopted, as one tolerance factor (called *intercalation factor* in this work), to gauge the geometrical mismatch of M<sub>6</sub>X block and A-site element. For the octahedra with side length of a, it can be shown that the height  $h = \frac{\sqrt{6}}{3}a$ ; and hence the size difference between M<sub>6</sub>X octahedra and A-site element can be expressed as:

$$\frac{\left|\frac{2}{3}\sqrt{6}R_M - R_A\right|}{\frac{2}{3}\sqrt{6}R_M}\tag{3}$$

Where  $R_M$  and  $R_A$  represent atomic radii of M-site elements and A-site elements respectively.

As shown in Fig. 2, there are n layers of  $M_6X$  octahedron separating each A- layer for  $M_{n+1}AX_n$  phases; that is, in 211 phases there is one  $M_6X$  octahedron layer; in 312 phases two  $M_6X$  octahedron layers, and in 413 phases three  $M_6X$  octahedron layers. Thus, the *intercalation factor* shown in Eq. (3) for 312 and 413 phases can be rewritten as  $\frac{\left|2*\frac{2}{3}\sqrt{6}R_M-R_A\right|}{2*\frac{2}{3}\sqrt{6}R_M}$  and  $\frac{\left|3*\frac{2}{3}\sqrt{6}R_M-R_A\right|}{3*\frac{2}{3}\sqrt{6}R_M}$ , respectively. In general, the *intercalation factor* for

 $M_{n+1}AX_n$  phases can be expressed as:

$$\frac{\left|n*\frac{2}{3}\sqrt{6}R_{M}-R_{A}\right|}{n*\frac{2}{3}\sqrt{6}R_{M}}\tag{4}$$

### 2.2 Introduction of octahedral factor

Further, by drawing lessens from tolerant factors designed for perovskites (*i.e.* another important type of Nowotny octahedral phases, but is a kind of valence compound), the *octahedral factor* is introduced in as the other tolerance factor [71-74]. For MAX phases, this is represented as:

$$\frac{R_X}{R_M} \tag{5}$$

Where  $R_X$  and  $R_M$  represent atomic radii of X-site elements and M-site elements respectively.

The *intercalation factor* and *octahedral factor*, shown in Eqs. (4) and (5), constitute the components of *new geometrical factor* (shown in Eq. (6)); which takes the sizes of M-, A-, X-sites elements and  $M_6X$  blocks, as well as the effect of stoichiometry factor, n, into consideration. Here, it worth noting that the geometrical factor is for characterization

of the lattice distortion, so that for alloys a linear combination of the sizes, with their stoichiometric ratios, of the constituent elements on M-, A- or X-site are employed.

New Geometrical Factor: 
$$\frac{\left|n*\frac{2}{3}\sqrt{6}R_{M}-R_{A}\right|}{n*\frac{2}{3}\sqrt{6}R_{M}} + \frac{R_{X}}{R_{M}}$$
 (6)

The values of atomic radii are taken from CRC Handbook [61]; and Table 2 listed the atomic radius values adopted in this work. In the next part, the *electron concentration* factor (shown in Eq. (2)) and new geometrical factor (shown in Eq. (6)) are employed to construct structure maps for framing out the formable regions of  $M_{n+1}AX_n$  phases.

Table 1 The valence/itinerant electron values adopted in this work [63, 66].

M-site		A-site		X-site	
Elements	Valence Electrons	Elements	Itinerant Electrons	Elements	Valence Electrons
Sc	3	Al	3.01	С	4
Ti	4	Si	4.00	N	5
V	5	P	4.97	В	5 3 5
Cr	6	$S^{**}$	6.00	P	5
Mn	7	Mn	1.05	S	6
Y	3	Fe	1.05	Se	6
Zr	4	Co	1.03		
Nb	5	Ni	1.16		
Mo	6	Cu	1.00		
Hf	4	Zn	2.04		
Ta	5	Ga	3.00		
$\mathbf{W}$	6	Ge	4.05		
Ce*	3	As	4.92		
Pr	2	Se**	6.00		
Nd	2	Rh	1.00		
Sm	2	Pd	0.96		
Gd	3	Ag	1.01		
Tb	2	Cd	2.03		
Dy	2 2	In	3.03		
Но		Sn	3.97		
Er	2	Sb	4.99		
Tm	2	Te**	6.00		
Yb	2	Ir	1.60		
Lu	3	Pt	1.63		
		Au	1.00		
		T1	3.03		
		Pb	4.00		
		Bi	4.94		

<sup>\*</sup>Due to the 4f orbitals penetrate the xenon core appreciably, they cannot overlap with ligand orbitals; and so, do not participate significantly in bonding [75]. Therefore, the 4f electrons of lanthanides are not counted.

<sup>\*\*</sup> Valence electrons are used

Table 2 The atomic radius values adopted in this work (Unit: Å) [61].

M-site		A-site		X-site	
Elements	Atomic Radius	Elements	Atomic Radius	Elements	Atomic Radius
Sc	1.59	Al	1.24	C	0.75
Ti	1.48	Si	1.14	N	0.71
V	1.44	P	1.09	В	0.84
Cr	1.30	S	1.04	P	1.09
Mn	1.29	Mn	1.29	S	1.04
Y	1.76	Fe	1.24	Se	1.18
Zr	1.64	Co	1.18		
Nb	1.56	Ni	1.17		
Mo	1.46	Cu	1.22		
Hf	1.64	Zn	1.20		
Ta	1.58	Ga	1.23		
W	1.50	Ge	1.20		
Ce	1.84	As	1.20		
Pr	1.90	Se	1.18		
Nd	1.88	Rh	1.34		
Sm	1.85	Pd	1.30		
Gd	1.82	Ag	1.36		
Tb	1.81	Cd	1.40		
Dy	1.80	In	1.42		
Но	1.79	Sn	1.40		
Er	1.77	Sb	1.40		
Tm	1.77	Te	1.37		
Yb	1.78	Ir	1.32		
Lu	1.74	Pt	1.30		
		Au	1.30		
		T1	1.44		
		Pb	1.45		
		Bi	1.50		

#### 3 Data collection

For constructing structure maps, the data of formable and non-formable MAX phases are collected. In this work, comprehensive but not exhaustive list of the experimental synthesized MAX phases (*i.e.* hypothetical MAX phases, like Sc<sub>2</sub>AlC, Y<sub>2</sub>AlC and Mo<sub>2</sub>AlC, are not included), which have definite compositions, are recorded as formable MAX phases (a total of 202 systems, shown in Table 3 and 4); and the ones that are screened based on elastic and thermodynamic stability by using *ab initio* calculations are recorded as non-formable MAX phases (a total of 92 systems, shown in Table 5) [26]. Here, the incentives of the choice for non-formable MAX phases are worth to be emphasized as follow.

It might be questioned that the non-formable phases are chosen based on the investigations without full stability calculations. It is acknowledged that there are valuable works that systematically investigate the stabilities of MAX phases *via* showing one given phase is more stable than all other competing phases [25, 29-31, 33], which brings a more rigorous criterion to discern possible MAX phases; and when done it properly, could screen potential MAX phases out showing excellent agreement with experimental observed ones [2]. Nevertheless, novel preparation strategies have recently been developed to synthesis MAX phases successfully *via* avoiding the reactions to form competitive phases [8, 10, 14, 76, 77]; and the adoptions of unstable phases derived from full stability computations would obstruct the classifications. In contrast, the two criteria employed by Aryal *et al.* [26] are necessary but not sufficient conditions for MAX phase formability; and the non-formable ones screened out by following these two criteria are the ones that would scarcely form.

Table 3 Comprehensive list of experimentally synthesized ternary MAX Phases<sup>a</sup>

Al		Si		P		S	
Ti <sub>2</sub> AlC	Ta <sub>3</sub> AlC <sub>2</sub>	Ti <sub>3</sub> SiC <sub>2</sub>		V <sub>2</sub> PC		Ti <sub>2</sub> SC	
$V_2AlC$	$Zr_3AlC_2$	Ti <sub>4</sub> SiC <sub>3</sub>		Nb <sub>2</sub> PC		$Zr_2SC$	
Cr <sub>2</sub> AlC	$Hf_3AlC_2$					$Nb_2SC$	
$Nb_2AlC$	Ti <sub>4</sub> AlN <sub>3</sub>					$Hf_2SC$	
Ta <sub>2</sub> AlC	Ta <sub>4</sub> AlC <sub>3</sub>					Zr <sub>2</sub> SB	
$Ti_2AlN$	$Nb_4AlC_3$					$Hf_2SB$	
$Zr_2AlC$	$V_4AlC_3$					$Nb_2SB$	
$Hf_2AlC$							
$Ti_3AlC_2$							
	~		~				~
	<del>Ja</del>		Ge		As		Se
Ti <sub>2</sub> GaC	V <sub>2</sub> GaN	Ti <sub>2</sub> GeC		V <sub>2</sub> AsC		Zr <sub>2</sub> SeC	
V <sub>2</sub> GaC	Sc <sub>2</sub> GaC	V <sub>2</sub> GeC		Nb <sub>2</sub> AsC		Hf <sub>2</sub> SeC	
Cr <sub>2</sub> GaC	Cr <sub>2</sub> GaN	Cr <sub>2</sub> GeC				Zr <sub>2</sub> SeB	
Nb <sub>2</sub> GaC	Ti <sub>3</sub> GaC <sub>2</sub>	Nb <sub>2</sub> GeC				Hf <sub>2</sub> SeB	
Mo <sub>2</sub> GaC	Ta <sub>4</sub> GaC <sub>3</sub>	Ti <sub>3</sub> GeC <sub>2</sub>				Zr <sub>2</sub> SeP	
Ta <sub>2</sub> GaC	Ti <sub>4</sub> GaC <sub>3</sub>	Ti <sub>4</sub> GeC <sub>3</sub>				Hf <sub>2</sub> SeP	
Mn <sub>2</sub> GaC							
Ti <sub>2</sub> GaN							
					G1		<b>D</b>
	<u>n</u>		Sn		Sb		Ге
Sc <sub>2</sub> InC	Zr <sub>2</sub> InN	Ti <sub>2</sub> SnC	$V_2SnC$	Ti <sub>2</sub> SbP		Zr <sub>2</sub> TeP	
Ti <sub>2</sub> InC	$Ti_3InC_2$	Hf <sub>2</sub> SnN	Sc <sub>2</sub> SnC	Zr <sub>2</sub> SbP			
Zr <sub>2</sub> InC		Zr <sub>2</sub> SnC	$Ti_3SnC_2$	Hf <sub>2</sub> SbP			
Nb <sub>2</sub> InC		Nb <sub>2</sub> SnC	$Zr_3SnC_2$	Nb <sub>2</sub> SbC			
Hf <sub>2</sub> InC		Hf <sub>2</sub> SnC	$Hf_3SnC_2$	Ti <sub>3</sub> SbC <sub>2</sub>			
Ti <sub>2</sub> InN		Lu <sub>2</sub> SnC					
	ΓΙ	Pb		Bi		Zn	
Ti <sub>2</sub> TlC	Zr <sub>2</sub> TlN	Ti <sub>2</sub> PbC	=	Nb <sub>2</sub> BiC		Ti <sub>2</sub> ZnC	Nb <sub>2</sub> ZnC
$Zr_2TlC$	212111	Zr <sub>2</sub> PbC		1,02210		Ti <sub>2</sub> ZnN	$Ti_3ZnC_2$
Hf <sub>2</sub> TlC		Hf <sub>2</sub> PbC				V <sub>2</sub> ZnC	$Ta_2ZnC$
2						. 2	2
Cu			C4	Iror	ı triad	Dwadan	is motals
Cu			Cd	(Fe,	Co, Ni)	Preciou	is metals
Ti <sub>2</sub> CuN		Ti <sub>2</sub> CdC		Ta <sub>2</sub> FeC	Nb <sub>2</sub> NiC	Mo <sub>2</sub> AuC	Ti <sub>3</sub> AuC <sub>2</sub>
Nb <sub>2</sub> CuC				Nb <sub>2</sub> FeC	Ta <sub>2</sub> NiC	Ti <sub>2</sub> AuN	
Ti <sub>4</sub> CuN <sub>3</sub>				Ti <sub>2</sub> FeN		Nb <sub>2</sub> AuC	
				Ta <sub>2</sub> CoC		Nb <sub>2</sub> PtC	
				Nb <sub>2</sub> CoC		Ti <sub>3</sub> IrC <sub>2</sub>	

<sup>&</sup>lt;sup>a</sup> This list is an updated version of list shown in Ref [7].

Table 4 List of experimentally synthesized MAX alloying phases<sup>a</sup>

	-		v 01				
	M	site	A site	X site			
211	$\begin{array}{l} (Ti_{0.02}Cr_{0.98})_2AlC\\ (Ti_{0.25}Cr_{0.75})_2AlC\\ (V_{0.65}Ta_{0.35})_2AlC\\ (V_{0.65}Ta_{0.35})_2AlC\\ (V_{0.65}Ta_{0.35})_2AlC\\ (Sc_{0.33}Nb_{0.67})_2AlC\\ (V_{0.96}Mn_{0.04})_2AlC\\ (Mo_{0.5}Mn_{0.5})_2GaC\\ (Cr_{0.5}Mn_{0.5})_2GaC\\ (Ti_{0.5}Zr_{0.5})_2InC\\ (Ti_{0.5}Hf_{0.5})_2InC\\ (Ti_{0.5}Hf_{0.5})_2InC\\ (Ti_{0.5}V_{0.5})_2GeC\\ (Cr_{0.5}Mn_{0.5})_2AuC\\ (Mo_{2/3}Sc_{1/3})_2AlC\\ (Mo_{2/3}Sc_{1/3})_2AlC\\ (Cr_{2/3}Y_{1/3})_2AlC\\ (Cr_{2/3}Y_{1/3})_2AlC\\ (W_{2/3}Sc_{1/3})_2AlC\\ (W_{2/3}Zr_{1/3})_2AlC\\ (V_{2/3}Zr_{1/3})_2AlC\\ (V_{2/3}Zr_{1/3})_2AlC\\ (V_{0.75}Cr_{0.25})_2AlC\\ (V_{0.25}Cr_{0.75})_2AlC\\ (V_{0.5}Cr_{0.5})_2AlC\\ (Cr_{0.5}V_{0.5})_2GeC\\ (Mo_{2/3}Gd_{1/3})_2AlC\\ (Cr_{0.5}V_{0.5}V_{0.5})_2GeC\\ (Mo_{2/3}Gd_{1/3})_2AlC\\ (Cr_{0.5}V_{0.5}V_{0.5})_2GeC\\ (Mo_{2/3}Gd_{1/3})_2AlC\\ (Cr_{0.5}V_{0.5}V_{0.5})_2GeC\\ (Mo_{2/3}Gd_{1/3})_2AlC\\ (Cr_{0.5}V_{0.5}V_{0.5})_2AlC\\ (Cr_{0.5}V_{0.$	(Mo2/3Ce1/3)2AlC (Mo2/3Pr1/3)2AlC (Mo2/3Nd1/3)2AlC (Mo2/3Sm1/3)2AlC (Mo2/3Tb1/3)2AlC (Mo2/3Tb1/3)2AlC (Mo2/3Dy1/3)2AlC (Mo2/3Er1/3)2AlC (Mo2/3Er1/3)2AlC (Mo2/3Er1/3)2AlC (Mo2/3F1/3)2AlC (Mo2/3Y1/3)2GaC (Mo2/3Y1/3)2GaC (Mo2/3Gd1/3)2GaC (Mo2/3Gd1/3)2GaC (Mo2/3Gd1/3)2GaC (Mo2/3F1/3)2GaC (Mo2/3F1/3)2GaC (Mo2/3F1/3)2GaC (Mo2/3F1/3)2GaC (Mo2/3F1/3)2GaC (Mo2/3Er1/3)2GaC (Mo2/3Er1/3)2GaC (Mo2/3Er1/3)2GaC (Mo2/3Er1/3)2GaC (Mo2/3Er1/3)2GaC (Mo2/3F1/3)2GaC (Mo2/3F1/3)2GaC (Mo2/3F1/3)2GaC (Mo2/3F1/3)2GaC (Mo2/3Lu1/3)2GaC (Mo2/3Lu1/3)2GaC (Ti0.25V0.75)2AlC (Ti0.25V0.75)2AlC (Ti0.5V0.5)2AlC	Nb <sub>2</sub> (Au <sub>0.5</sub> Al <sub>0.5</sub> )C Nb <sub>2</sub> (Ag <sub>0.3</sub> Sb <sub>0.4</sub> Al <sub>0.3</sub> )C Nb <sub>2</sub> (Pd <sub>0.5</sub> Sn <sub>0.5</sub> )C Nb <sub>2</sub> (Rh <sub>0.2</sub> Sn <sub>0.4</sub> Al <sub>0.4</sub> )C Nb <sub>2</sub> (Ge <sub>0.8</sub> Al <sub>0.2</sub> )C Zr <sub>2</sub> (Al <sub>0.42</sub> Bi <sub>0.58</sub> )C Cr <sub>2</sub> (Al <sub>0.9</sub> 7Si <sub>0.03</sub> )C Zr <sub>2</sub> (Al <sub>0.3</sub> Sb <sub>0.7</sub> )C Zr <sub>2</sub> (Al <sub>0.3</sub> 5Pb <sub>0.65</sub> )C Mo <sub>2</sub> (Ga <sub>0.33</sub> Fe <sub>0.5</sub> Au <sub>0.16</sub> )C	$Zr_2Se(B_{0.94}Se_{0.06})$ $Zr_2Se(B_{0.93}Se_{0.07})$ $Zr_2Se(B_{0.89}Se_{0.11})$ $Zr_2Se(B_{0.83}Se_{0.17})$ $Zr_2Se(B_{0.64}Se_{0.36})$ $Zr_2Se(B_{0.40}Se_{0.60})$ $Zr_2Se(B_{0.03}Se_{0.97})$			
312	$\begin{array}{c} (Cr_{2/3}Ti_{1/3})_3AlC_2\\ (Cr_{2/3}V_{1/3})_3AlC_2\\ (Mo_{2/3}Ti_{1/3})_3AlC_2\\ (Mo_{2/3}Sc_{1/3})_3AlC_2\\ \end{array}$		$\begin{array}{c} Ti_3(Sb_{0.5}Sn_{0.5})CN \\ Ti_3(Sb_{0.5}Sn_{0.5})C_2 \\ Ti_3(Cd_{0.5}Zn_{0.5})C_2 \\ Ti_3(Al_{0.8}Sn_{0.2})C_2 \\ Ta_3(Al_{0.96}Sn_{0.04})C_2 \end{array}$	Ti <sub>3</sub> SbCN Ti <sub>3</sub> AlCN Ti <sub>3</sub> SnCN Ti <sub>3</sub> GaCN			
413	$\begin{array}{c} (Nb_{0.5}V_{0.5})_4AlC_3\\ (Nb_{0.8}Ti_{0.2})_4AlC_3\\ (Nb_{0.8}Zr_{0.2})_4AlC_3\\ (Cr_{5/8}Ti_{3/8})_4AlC_3\\ (V_{0.5}Cr_{0.5})_4AlC_3\\ (Mo_{0.5}Ti_{0.5})_4AlC_3\\ \end{array}$						

<sup>&</sup>lt;sup>a</sup> This list is an updated version of lists shown in Ref [7] and [33].

Table 5 List of non-formable MAX phase screened via ab initio calculations [26].

211		312			413	
Cr <sub>2</sub> InC	Mo <sub>2</sub> GaN	Cr <sub>3</sub> InC <sub>2</sub>	$Mo_3InN_2$	Cr <sub>4</sub> GaC <sub>3</sub>	Mo <sub>4</sub> AsC <sub>3</sub>	
$Cr_2TlC$	$Mo_2InN$	$Cr_3TlC_2$	$Mo_3TlN_2$	Cr <sub>4</sub> InC <sub>3</sub>	$Mo_4SC_3$	
$Cr_2SnC$	$Mo_2TlN$	$Cr_3GeC_2$	$Mo_3SiN_2$	Cr <sub>4</sub> TlC <sub>3</sub>	$V_4PbN_3$	
$Cr_2PbC$	$Mo_2SiN$	$Cr_3SnC_2$	$Mo_3GeN_2$	Cr <sub>4</sub> SiC <sub>3</sub>	$Ta_4TlN_3$	
$Cr_2SC$	$Mo_2GeN$	$Cr_3PbC_2$	$Mo_3SnN_2$	Cr <sub>4</sub> GeC <sub>3</sub>	$Ta_4PbN_3$	
$Mo_2InC$	$Mo_2PbN$	Cr <sub>3</sub> AsC <sub>2</sub>	$Mo_3PbN_2$	Cr <sub>4</sub> SnC <sub>3</sub>	Cr <sub>4</sub> SiN <sub>3</sub>	
$Mo_2TlC$	$Mo_2PN$	$Mo_3GaC_2$	$Mo_3PN_2$	Cr <sub>4</sub> PbC <sub>3</sub>	$Cr_4PbN_3$	
$Mo_2SnC$	$Mo_2AsN$	$Mo_3InC_2$	$Mo_3AsN_2$	Cr <sub>4</sub> PC <sub>3</sub>	$Cr_4PN_3$	
$Mo_2PbC$		$Mo_3TlC_2$		Cr <sub>4</sub> AsC <sub>3</sub>	$Cr_4SN_3$	
$Mo_2SC$		Mo <sub>3</sub> SiC <sub>2</sub>		Cr <sub>4</sub> SC <sub>3</sub>	$Mo_4GaN_3$	
$V_2SN$		$Mo_3GeC_2$		Mo <sub>4</sub> AlC <sub>3</sub>	$Mo_4InN_3$	
Nb <sub>2</sub> GaN		$Mo_3SnC_2$		Mo <sub>4</sub> GaC <sub>3</sub>	$Mo_4T1N_3$	
$Nb_2SN$		$Mo_3PbC_2$		Mo <sub>4</sub> InC <sub>3</sub>	$Mo_4SiN_3$	
$Ta_2InN$		$Mo_3AsC_2$		Mo <sub>4</sub> TlC <sub>3</sub>	$Mo_4GeN_3$	
Ta <sub>2</sub> GeN		$Mo_3SC_2$		Mo <sub>4</sub> SiC <sub>3</sub>	$Mo_4SnN_3$	
$Cr_2TlN$		$Ta_3PbN_2$		Mo <sub>4</sub> GeC <sub>3</sub>	$Mo_4PbN_3$	
$Cr_2PbN$		Cr <sub>3</sub> PN <sub>2</sub>		Mo <sub>4</sub> SnC <sub>3</sub>	$Mo_4PN_3$	
$Cr_2PN$		$Mo_3AlN_2$		Mo <sub>4</sub> PbC <sub>3</sub>	$Mo_4AsN_3$	
Mo <sub>2</sub> AlN		Mo <sub>3</sub> GaN <sub>2</sub>		Mo <sub>4</sub> PC <sub>3</sub>	Mo <sub>4</sub> SN <sub>3</sub>	

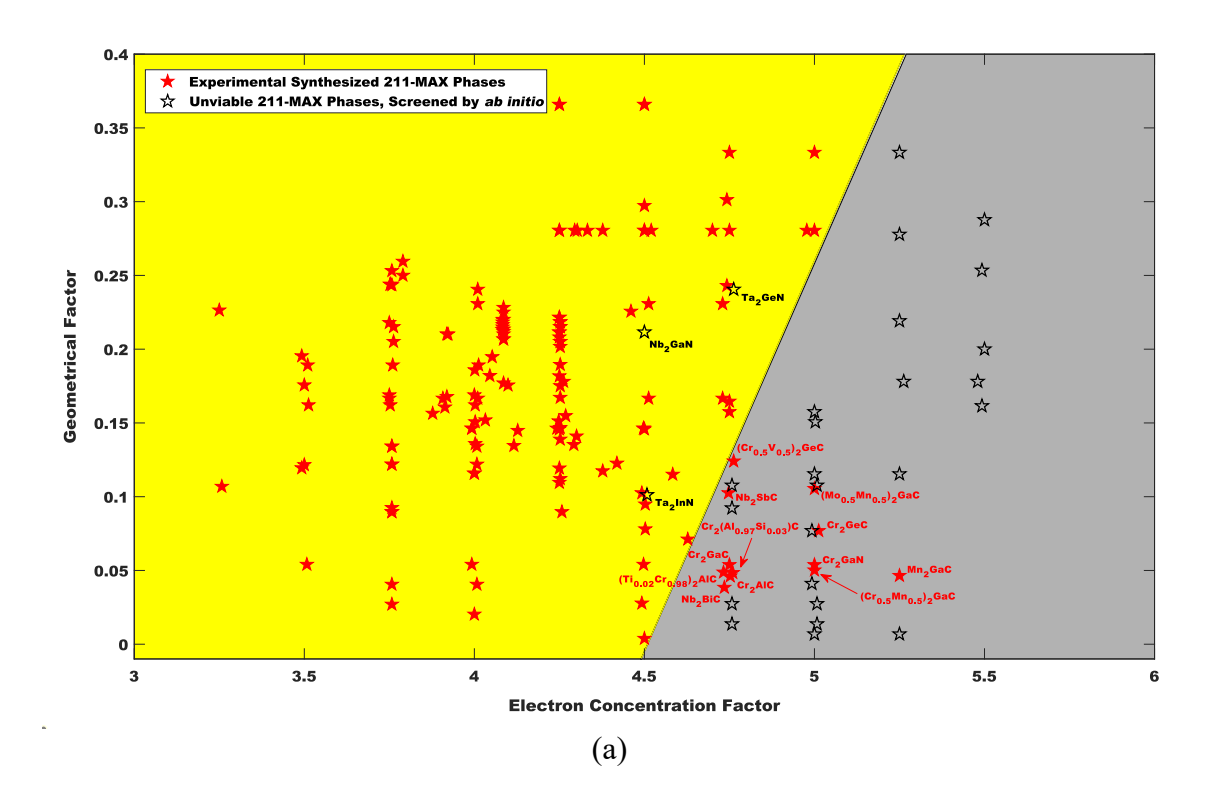
### 4 Results and discussion

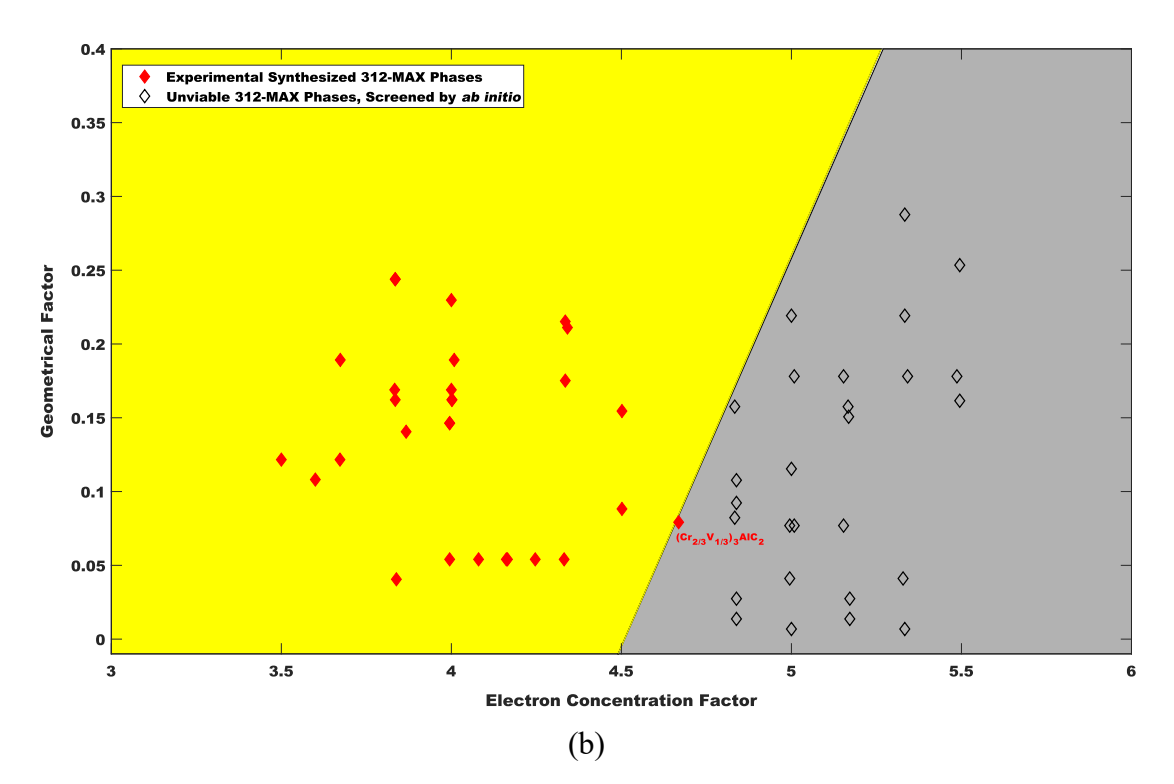
### 4.1 The structure maps construction for MAX phases formability

Firstly, the quest for generality raises the inquiry of whether the *geometrical* and *electron concentration* factors proposed in Ref. [6] could be extended to a broad family of M<sub>n+1</sub>AX<sub>n</sub> phases; and Fig. 3 (a)-(c) show the constructed structure maps through *geometrical* and *electron concentration* factors proposed in Ref. [6] for 211-MAX phases, 312-MAX phases and (c) 413-MAX phases respectively, where the outliers are marked with labels of corresponding compositions. It is shown that, with fidelity of 92.1%, the applications of the *geometrical* and *electron concentration* factors proposed *in prior* to broad MAX-phase members are feasible. Nevertheless, it is expected to further enhance the fidelity through upgrading the expressions of *geometrical* factor, by taking the X-site elements dimension, as well as different *n* values, into considerations.

The renewal structure maps of MAX phases formability are constructed from Eqn. (2) and Eqn. (6), which are shown in Fig. 4-6 for 211-, 312- and 413-MAX phases respectively (The structure maps with full set of labels are shown in S1-S3 in Supplement

Information). It can be found that, only with a few exceptions, the points representing formable MAX phases and those of non-formable ones are located within two separable regions; and successful formability/non-formability separation is achieved with a fidelity of 95.5%.





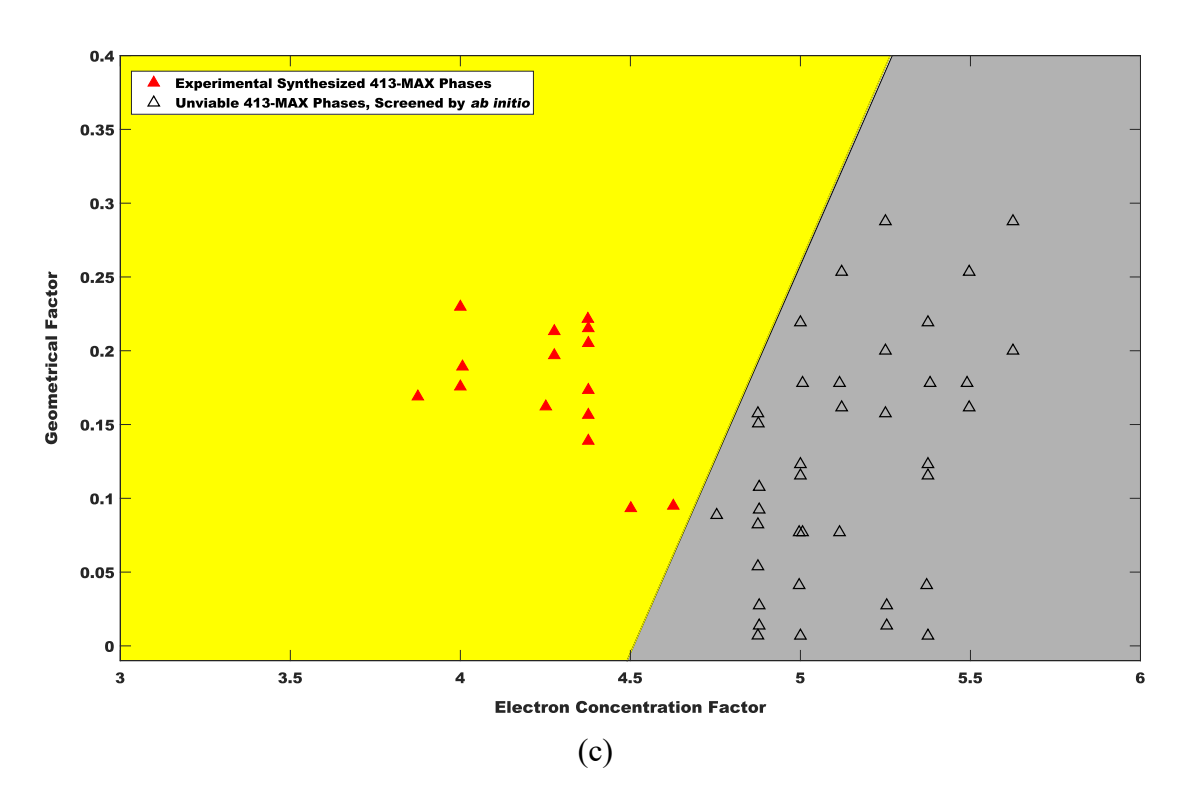


Fig. 3 The structure maps constructed *via* geometrical and electron concentration factors proposed in Ref. [6] for (a) 211-MAX phases; (b) 312-MAX phases; and (c) 413-MAX phases

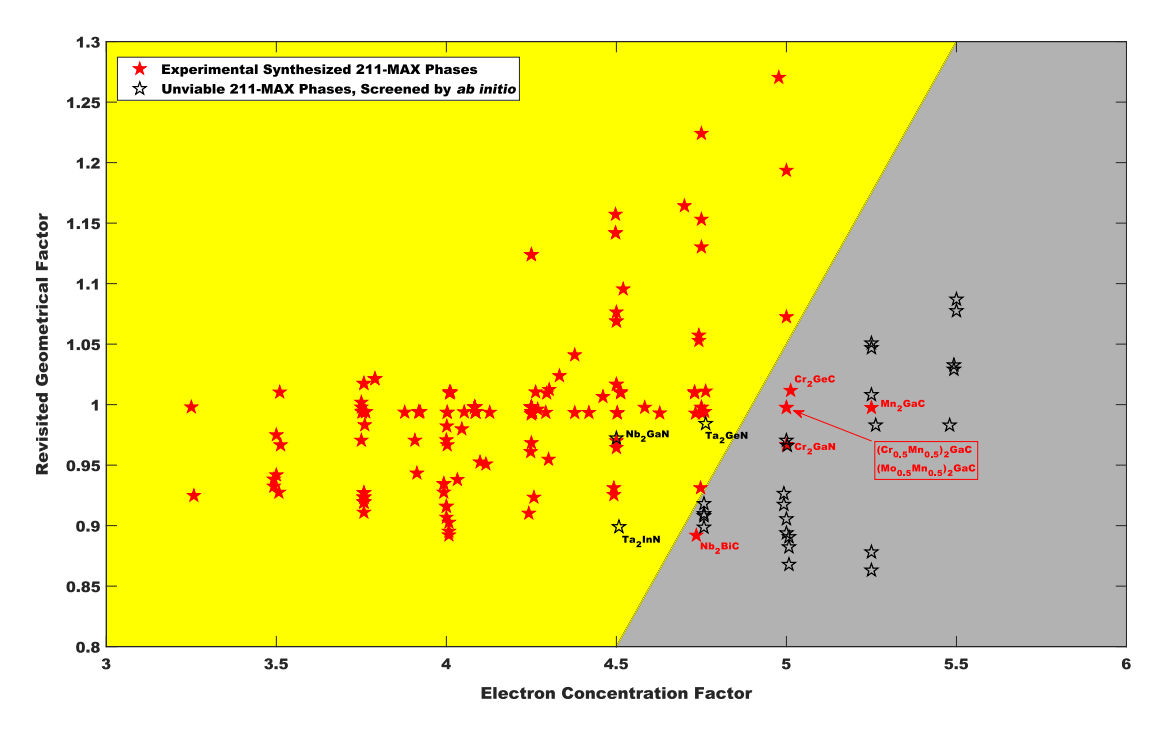


Fig. 4 The structure maps constructed *via* revisited geometrical and electron concentration factors for (a) 211-MAX phases (ternary) and (b) 211-MAX alloying phases.

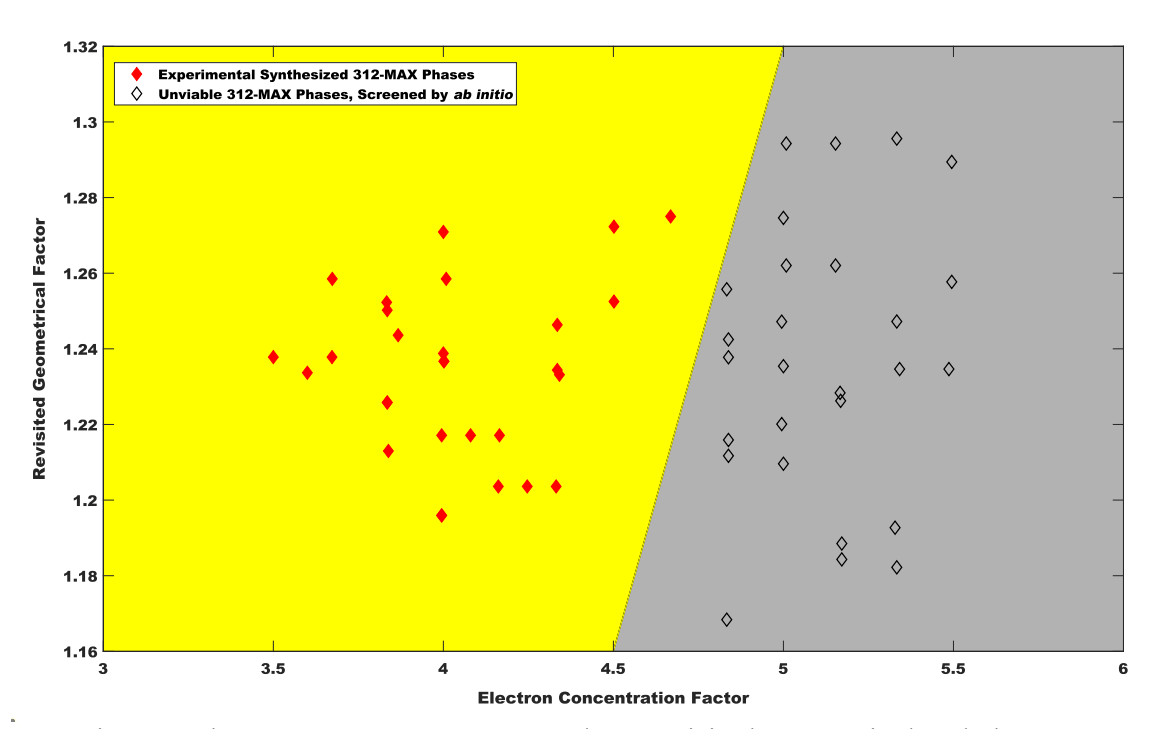


Fig. 5 The structure maps constructed *via* revisited geometrical and electron concentration factors for 312-MAX phases.

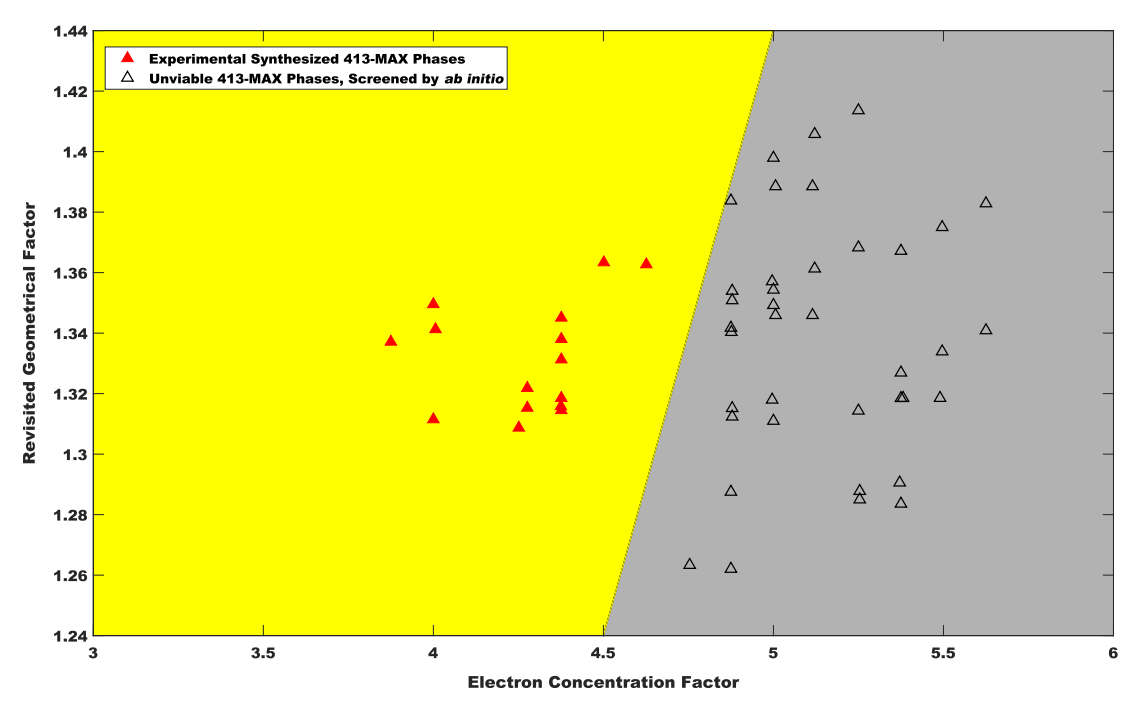


Fig. 6 The structure maps constructed *via* revisited geometrical and electron concentration factors for 413-MAX phases.

# 4.2 The MAX phases with high electron concentration elements and the effects of geometrical factor and alloying

In Fig. 4, it is shown that several synthesized Cr-, Mn- and Nb- containing 211-MAX phases (*i.e.* Cr<sub>2</sub>GeC, Cr<sub>2</sub>GaN, Mn<sub>2</sub>GaC, Nb<sub>2</sub>BiC, (Mo<sub>0.5</sub>Mn<sub>0.5</sub>)<sub>2</sub>GaC, (Cr<sub>0.5</sub>Mn<sub>0.5</sub>)<sub>2</sub>GaC) locate within the non-formable region. In Barsoum's monograph, the phases associated with high electron concentrations are fully discussed and referred as anomalous or borderline-stable compounds; where the phases of Cr<sub>2</sub>GeC, Cr<sub>2</sub>AlC and V<sub>2</sub>AsC are taken as examples [2].

However, the geometrical factor plays an important role in offsetting the destabilizing effect of electron concentration factor, when taking the MAX phases containing Mo- as examples. The formability/non-formability of Mo- containing phases are distinctly separated, where the formability of Mo<sub>2</sub>GaC could be attributed to its geometrical factor. In addition, due to the contributions from geometrical factors of

Cr<sub>2</sub>AlC and V<sub>2</sub>AsC, these two mentioned borderline-stable compounds are properly classified as formable ones.

Further, it is shown that the alloying also imposes stabilizing effects *via* tuning the electron concentrations. For example, the compounds of Cr<sub>3</sub>AlC<sub>2</sub> and Mo<sub>3</sub>AlC<sub>2</sub> do not exist [78], but (Cr<sub>2/3</sub>Ti<sub>1/3</sub>)<sub>3</sub>AlC<sub>2</sub> [79], (Cr<sub>2/3</sub>V<sub>1/3</sub>)<sub>3</sub>AlC<sub>2</sub> [80], (Mo<sub>2/3</sub>Ti<sub>1/3</sub>)<sub>3</sub>AlC<sub>2</sub> [81] and (Mo<sub>2/3</sub>Sc<sub>1/3</sub>)<sub>3</sub>AlC<sub>2</sub> [82] have been successfully synthesized. In addition, while the Mo<sub>4</sub>AlC<sub>3</sub> phase is screened out as non-formable one, (Mo<sub>0.5</sub>Ti<sub>0.5</sub>)<sub>4</sub>AlC<sub>3</sub> has been derived experimentally [82].

## 4.3 The validity of electron concentration and geometrical factors

From the results depicted in Fig. 4-6, it is found that in 2D *electron concentration* factor vs. geometrical factor maps, the formable and non-formable MAX phases tend to cluster in separated regions. Accordingly, the distinguishing power for formable and non-formable of MAX phases from the compounding effect of *electron concentration* and geometrical factor can be fully acknowledged.

However, the *geometrical factor* suffers from relying heavily on empirical atomic radii. It is well known that the atomic radii in compounding state is not precisely defined and that even within the same definition there are variations reflecting the coordination and local chemistry [83-87]. Due to these uncertainties transfer to the *intercalation* and *octahedral* factors, the predictive power for future MAX phases might be weaken. To overcome these limitations, precise atomic radii determined from first principles should be introduced.

For *electron concentration* factor, the number of valence electrons is applied to M-site elements, by considering the covalent characteristic of M-X bonding. However, the heterodesmic characteristics possessed by M-site elements (where M-X bonding is

covalent, and M-A bonding is metallic) requires further elaborations for the choice of electron concentration parameters [65].

# 4.4 The gap in the capability of distinction for the chemical order and disorder

The families of MAX phases have significantly expanded within last few years, in particular for the quaternary and even quinary phases are derived upon alloying. In 2014, one chemically ordered MAX phase, *i.e.* Cr<sub>2</sub>TiAlC<sub>2</sub>, was reported [79], which displays out-of-plane order from alternating layers composed of one M element only. Other out-of-plane ordered MAX phases then followed soon [80-82]. In 2017, MAX phases with in-plane ordering of M-site elements of a 2:1 ratio were discovered [88, 89]. Further, the expansions of MAX phase members have also been manifested through complete or partial substation on the A-site elements [8, 90-96].

It is well acknowledged that, the understanding of why certain metal combinations would lead to the formation of i-MAX, o-MAX or solid solution phases is a fundamental question. Recently, Dahlqvist and Rosen [33] has carried out an assessment for identifying the formation rules defining the preference for chemical order (i-MAX phase) or disorder (solid solution), by employing energy difference calculations on 2702 unique compositions. In contrast, the present work mainly focuses on making the robust and efficient associations between the chemical formular of  $M_{n+1}AX_n$  to the structure type of MAX phases; and another classification theme should be built for further distinguishing the phases with chemical order and disorder.

# 4.5 What is the generality belongs to: the *proposed factors* or the *developed maps*?

In recent times, we have noticed Carlsson *et al.* [30] have challenged the use of structure mapping for identifying formable MAX phases [6, 15]. We are fully appreciated

the critical assessments imposed on our developed strategy; however, several notions have to be illuminated here. Firstly, the developed structure map is aiming for mapping MAX phase structures to their compositions with chemical formular expression of  $M_{n+1}AX_n$ , on which the lines that distinguish the formable regions are defined. While in Carlsson et al.'s work, they directly applied the defined lines on the case of MAB phases, with chemical formulas of MAB, M<sub>2</sub>AB<sub>2</sub>, M<sub>3</sub>AB<sub>4</sub>, M<sub>4</sub>AB<sub>4</sub> and M<sub>4</sub>AB<sub>6</sub>, all of which have different chemical formula style from  $M_{n+1}AX_n$ . Therefore, the developed structure map in Ref. [6], as well as the defined lines to distinguish the formable regions, cannot applied directly. Secondly, Carlsson et al. have put all the orthorhombic and hexagonal MAB phases (that with different chemical formular styles) together for mapping the phase stable region. It has to be emphasized that compounds with different chemical formular styles cannot be put together, and separate mappings have to be conducted for each chemical formular style. Thirdly, the Fig. S15-S19 in Carlsson et al.'s work shows the mappings for each considered composition (i.e. MAB, M<sub>2</sub>AB<sub>2</sub>, M<sub>3</sub>AB<sub>4</sub>, M<sub>4</sub>AB<sub>4</sub> and M<sub>4</sub>AB<sub>6</sub>) separately, where the visible separations can be seen. Therefrom the lines for distinguishing the formable regions can be derived accordingly for each case. Based on above analysis, there are the generalities that proposed factors have, but not belong to the developed maps that are specific for  $M_{n+1}AX_n$  phases.

### 5 Conclusions

As one kind of heterodesmic compounds, MAX phases possess chemical bonding of metallic, ionic, covalent, or a changing mixture of those. Conventionally, the explorations of the uncharted territories of MAX phases, with respect to their composition and structure, demand conducting of trail-and-error experimentations or analytical solutions of Schrödinger equations. These tactics have shown their values in determining

given MAX phases; yet, the intensive characteristics restrict their efficiencies for future candidate investigations. In this work, we have employed phenomenological structure mapping strategy to develop a classification scheme, with a fidelity of 95.5%, for MAX phases formability/non-formability separation. More generally, current findings suggest that the proposed genomic blueprints, that is *geometrical* and *electron concentration* factors, could serve as a powerful tool to tackle the factorial complexity of combinatorial MAX phases design.

# Acknowledgement

The authors acknowledge the financial support of Pioneer and Leading Goose R&D Program of Zhejiang (No. 2022C01236), National Natural Science Foundation of China (No. 52250005, U2004212), and Ten-Thousand Talents Plan of Zhejiang Province (No. 2022R51007).

## References

- [1] M.W. Barsoum, The M<sub>N+1</sub>AX<sub>N</sub> phases: A new class of solids: Thermodynamically stable nanolaminates, Prog. Solid State Chem. 28 (2000) 201-281.
- [2] M.W. Barsoum, MAX Phases: Properties of Machinable Ternary Carbides and Nitrides, Wiley-VCH, Weinheim, 2013.
- [3] P. Eklund, M. Beckers, U. Jansson, H. Högberg, L. Hultman, The M<sub>n+1</sub>AX<sub>n</sub> phases: Materials science and thin-film processing, Thin Solid Films 518 (2010) 1851-1878.
- [4] N. Goossens, B. Tunca, T. Lapauw, K. Lambrinou, J. Vleugels, MAX Phases, Structure, Processing, and Properties, in: M. Pomeroy (Ed.), Encyclopedia of Materials: Technical Ceramics and Glasses, Elsevier, Oxford, 2021, pp. 182-199.
- [5] H. Ding, M. Li, Y. Li, K. Chen, Y. Xiao, J. Zhou, Q. Thao, J. Rosen, H. Yin, Y. Bai,

- B. Zhang, Z. Sun, J. Wang, Y. Zhang, Z. Huang, P. Zhang, Z. Sun, M. Han, S. Zhao,C. Wang, Q. Huang, Progress in structural tailoring and properties of ternary layered materials, J. Inorg. Mater. (2023) DOI: 10.15541/jim20230123.
- [6] Y. Zhang, Z. Mao, Q. Han, Y. Li, M. Li, S. Du, Z. Chai, Q. Huang, The role of Hume-Rothery's rules play in the MAX phases formability, Materialia 12 (2020) 100810.
- [7] M. Sokol, V. Natu, S. Kota, M.W. Barsoum, On the chemical diversity of the MAX phases, Trends Chem. 1 (2019) 210-223.
- [8] Y.B. Li, J. Lu, M. Li, K.K. Chang, X.H. Zha, Y.M. Zhang, K. Chen, P.O.A. Persson, L. Hultman, P. Eklund, S.Y. Du, J.S. Francisco, Z.F. Chai, Z.R. Huang, Q. Huang, Multielemental single atom-thick A layers in nanolaminated V<sub>2</sub>(Sn, A)C (A = Fe, Co, Ni, Mn) for tailoring magnetic properties, PNAS 117 (2020) 820-825.
- [9] Y.B. Li, G.L. Ma, H. Shao, P. Xiao, J. Lu, J. Xu, J.R. Hou, K. Chen, X. Zhang, M. Li, P.O.A. Persson, L. Hultman, P. Eklund, S.Y. Du, Z.F. Chai, Z.R. Huang, N. Jin, J.W. Ma, Y. Liu, Z.F. Lin, Q. Huang, Electrochemical lithium storage performance of molten salt derived V<sub>2</sub>SnC MAX Phase, Nano Micro Lett. 13 (2021) 158.
- [10] Y.B. Li, Y.Q. Qin, K. Chen, L. Chen, X. Zhang, H.M. Ding, M. Li, Y.M. Zhang, S.Y. Du, Z.F. Chai, Q. Huang, Molten salt synthesis of nanolaminated Sc<sub>2</sub>SnC MAX phase, J. Inorg. Mater. 36 (2021) 773-778.
- [11] K. Chen, X.J. Bai, X.L. Mu, P.F. Yan, N.X. Qiu, Y.B. Li, J. Zhou, Y.J. Song, Y.M. Zhang, S.Y. Du, Z.F. Chai, Q. Huang, MAX phase Zr<sub>2</sub>SeC and its thermal conduction behavior, J. Eur. Ceram. Soc. 41 (2021) 4447-4451.
- [12] K. Chen, X.D. Wang, J.N. Zhang, H.M. Ding, Y.B. Li, Y.J. Song, F.F. Ge, X.B. Zhou, S.Y. Du, Q. Huang, Effect of A-site atom on static corrosion behavior and irradiation damage of Ti<sub>2</sub>SC phases, J. Am. Ceram. Soc. 105 (2022) 1386-1393.
- [13] X.D. Wang, K. Chen, E.X. Wu, Y.M. Zhang, H.M. Ding, N.X. Qiu, Y.J. Song, S.Y.

- Du, Z.F. Chai, Q. Huang, Synthesis and thermal expansion of chalcogenide MAX phase Hf<sub>2</sub>SeC, J. Eur. Ceram. Soc. 42 (2022) 2084-2088.
- [14] H. Ding, Y. Li, M. Li, K. Chen, K. Liang, G. Chen, J. Lu, J. Palisaitis, P.O.A. Persson, P. Eklund, L. Hultman, S. Du, Z. Chai, Y. Gogotsi, Q. Huang, Chemical scissormediated structural editing of layered transition metal carbides, Science 379 (2023) 1130-1135.
- [15] C. Shen, Q. Gao, N.M. Fortunato, H.K. Singh, I. Opahle, O. Gutfleisch, H.B. Zhang, Designing of magnetic MAB phases for energy applications, J. Mater. Chem. A 9 (2021) 8805-8813.
- [16] Y. Zhou, H. Xiang, C. Hu, Extension of MAX phases from ternary carbides and nitrides (X = C and N) to ternary borides (X = B, C, and N): A general guideline, Int. J. Appl. Ceram. Technol. 20 (2023) 803-822.
- [17] T. Rackl, D. Johrendt, The MAX phase borides Zr<sub>2</sub>SB and Hf<sub>2</sub>SB, Solid State Sci. 106 (2020) 106316.
- [18] L. Chen, Y.B. Li, K. Chen, X.J. Bai, M.A. Li, S.Y. Du, Z.F. Chai, Q. Huang, Synthesis and characterization of medium-/high-entropy M<sub>2</sub>SnC (M=Ti/V/Nb/Zr/Hf) MAX Phases, Small Struct. 4 (2022) 2200161.
- [19] S. Zhao, L. Chen, H. Xiao, J. Huang, Y.X. Li, Y.Z. Qian, T. Zheng, Y.B. Li, L.X. Cao, H. Zhang, H.C. Liu, Y.G. Wang, Q. Huang, C.X. Wang, Phase transformation and amorphization resistance in high-entropy MAX phase M<sub>2</sub>SnC ( M = Ti, V, Nb, Zr, Hf) under in-situ ion irradiation, Acta Mater. 238 (2022) 118222.
- [20] Z.Q. Li, E.X. Wu, K. Chen, X.D. Wang, G.X. Chen, L.J. Miao, Y.M. Zhang, Y.J. Song, S.Y. Du, Z.F. Chai, Q. Huang, Chalcogenide MAX phases Zr<sub>2</sub>Se(B<sub>1-x</sub>Se<sub>x</sub>) (x=0-0.97) and their conduction behaviors, Acta Mater. 237 (2022) 118183.
- [21] J. Halim, A.S. Etman, A. Elsukova, P. Polcik, J. Palisaitis, M.W. Barsoum, P.O.Å.

- Persson, J. Rosen, Tailored synthesis approach of (Mo<sub>2/3</sub>Y<sub>1/3</sub>)<sub>2</sub>AlC i-MAX and its two-dimensional derivative Mo<sub>1.33</sub>CT<sub>z</sub> MXene: enhancing the yield, quality, and performance in supercapacitor applications, Nanoscale 13 (2021) 311-319.
- [22] J. Thörnberg, J. Halim, J. Lu, R. Meshkian, J. Palisaitis, L. Hultman, P.O.Å. Persson, J. Rosen, Synthesis of (V<sub>2/3</sub>Sc<sub>1/3</sub>)<sub>2</sub>AlC i-MAX phase and V<sub>2-x</sub>C MXene scrolls, Nanoscale 11 (2019) 14720-14726.
- [23] M.F. Cover, O. Warschkow, M.M.M. Bilek, D.R. McKenzie, A comprehensive survey of M<sub>2</sub>AX phase elastic properties, J. Phys.: Condens. Matter 21 (2009) 305403.
- [24] V.J. Keast, S. Harris, D.K. Smith, Prediction of the stability of the M<sub>n+1</sub>AX<sub>n</sub> phases from first principles, Phys. Rev. B 80 (2009) 214113.
- [25] M. Dahlqvist, B. Alling, J. Rosén, Stability trends of MAX phases from first principles, Phys. Rev. B 81 (2010) 220102(R).
- [26] S. Aryal, R. Sakidja, M.W. Barsoum, W.-Y. Ching, A genomic approach to the stability, elastic, and electronic properties of the MAX phases, Phys. Status Solidi B 251 (2014) 1480-1497.
- [27] D. Ohmer, I. Opahle, H.K. Singh, H. Zhang, Stability predictions of magnetic M<sub>2</sub>AX compounds, J. Phys.: Condens. Matter 31 (2019) 405902.
- [28] D. Ohmer, G. Qiang, I. Opahle, H.K. Singh, H. Zhang, High-throughput design of 211-M<sub>2</sub>AX compounds, Phys. Rev. Materials 3 (2019) 053803.
- [29] M. Ashton, R.G. Hennig, S.R. Broderick, K. Rajan, S.B. Sinnott, Computational discovery of stable M<sub>2</sub>AX phases, Phys. Rev. B 94 (2016) 054116.
- [30] A. Carlsson, J. Rosen, M. Dahlqvist, Theoretical predictions of phase stability for orthorhombic and hexagonal ternary MAB phases, Phys. Chem. Chem. Phys. 24 (2022) 11249-11258.

- [31] M. Dahlqvist, J. Rosen, Predictive theoretical screening of phase stability for chemical order and disorder in quaternary 312 and 413 MAX phases, Nanoscale 12 (2020) 785-794.
- [32] R. Khaledialidusti, M. Khazaei, S. Khazaei, K. Ohno, High-throughput computational discovery of ternary-layered MAX phases and prediction of their exfoliation for formation of 2D MXenes, Nanoscale 13 (2021) 7294-7307.
- [33] M. Dahlqvist, J. Rosen, The rise of MAX phase alloys large-scale theoretical screening for the prediction of chemical order and disorder, Nanoscale 14 (2022) 10958-10971.
- [34] S. Li, Z. Yang, R. Khaledialidusti, S. Lin, J. Yu, M. Khazaei, J. Zhang, L. Sun, X. Li, W. Sun, High-throughput study and machine learning on MAX and MAB phases: new materials and fingerprints of superior lattice thermal conductivities, Acta Mater. 254 (2023) 119001.
- [35] D.G. Pettifor, The structures of binary compounds. I. Phenomenological structure maps, J. Phys. C: Solid State Phys. 19 (1986) 285-313.
- [36] D.G. Pettifor, A chemical scale for crystal-structure maps, Solid State Commun. 51 (1984) 31-34.
- [37] D.G. Pettifor, Structure mapping, in: J.H. Westbrook, R.L. Fleischer (Eds.), Crystal Structures of Intermetallic Compounds, Wiley, Chichester, 2000, pp. 195-214.
- [38] D.G. Pettifor, Structure maps revisited, J. Phys.: Condens. Matter 15 (2003) V13-V16.
- [39] D.G. Pettifor, Structure maps in alloy design, J. Chem. Soc., Faraday Trans. 86 (1990) 1209-1213.
- [40] D.G. Pettifor, Structure maps in magnetic alloy design, Physica B&C 149 (1988) 3-10.

- [41] D.G. Pettifor, Structure maps for pseudobinary and ternary phases, Mater. Sci. Technol. 4 (1988) 675-691.
- [42] D.G. Pettifor, Structure maps for ordered intermetallics, Nato Advanced Research Workshop on Ordered Intermetallics: Physical Metallurgy and Mechanical Behavior, Irsee, Germany, 1991, pp. 47-59.
- [43] W. Hume-Rothery, The Engel-Brewer theories of metals and alloys, Prog. Mater Sci. 13 (1968) 229-265.
- [44] E. Mooser, W.B. Pearson, On the crystal chemistry of normal valence compounds, Acta Cryst. 12 (1959) 1015-1022.
- [45] J.C. Phillips, Vanvecht.Ja, Dielectric classification of crystal structures ionization potentials and band structures, Phys. Rev. Lett. 22 (1969) 705-708.
- [46] A. Zunger, Structural stability of 495 binary compounds, Phys. Rev. Lett. 44 (1980) 582-586.
- [47] C.S. Kong, W. Luo, S. Arapan, P. Villars, S. Iwata, R. Ahuja, K. Rajan, Information-theoretic approach for the discovery of design rules for crystal chemistry, J. Chem. Inf. Model. 52 (2012) 1812-1820.
- [48] C. Sun Kong, P. Villars, S. Iwata, K. Rajan, Mapping the 'materials gene' for binary intermetallic compounds—a visualization schema for crystallographic databases, Comput. Sci. Discovery 5 (2012) 015004.
- [49] P. Villars, A three-dimensional structural stability diagram for 1011 binary AB<sub>2</sub> intermetallic compounds: II, J. Less-Common Met. 99 (1984) 33-43.
- [50] P. Villars, Three-dimensional structural stability diagrams for 648 binary AB<sub>3</sub> and 389 binary A<sub>3</sub>B<sub>5</sub> intermetallic compounds: III, J. Less-Common Met. 102 (1984) 199-211.
- [51] P. Villars, A three-dimensional structural stability diagram for 998 binary AB

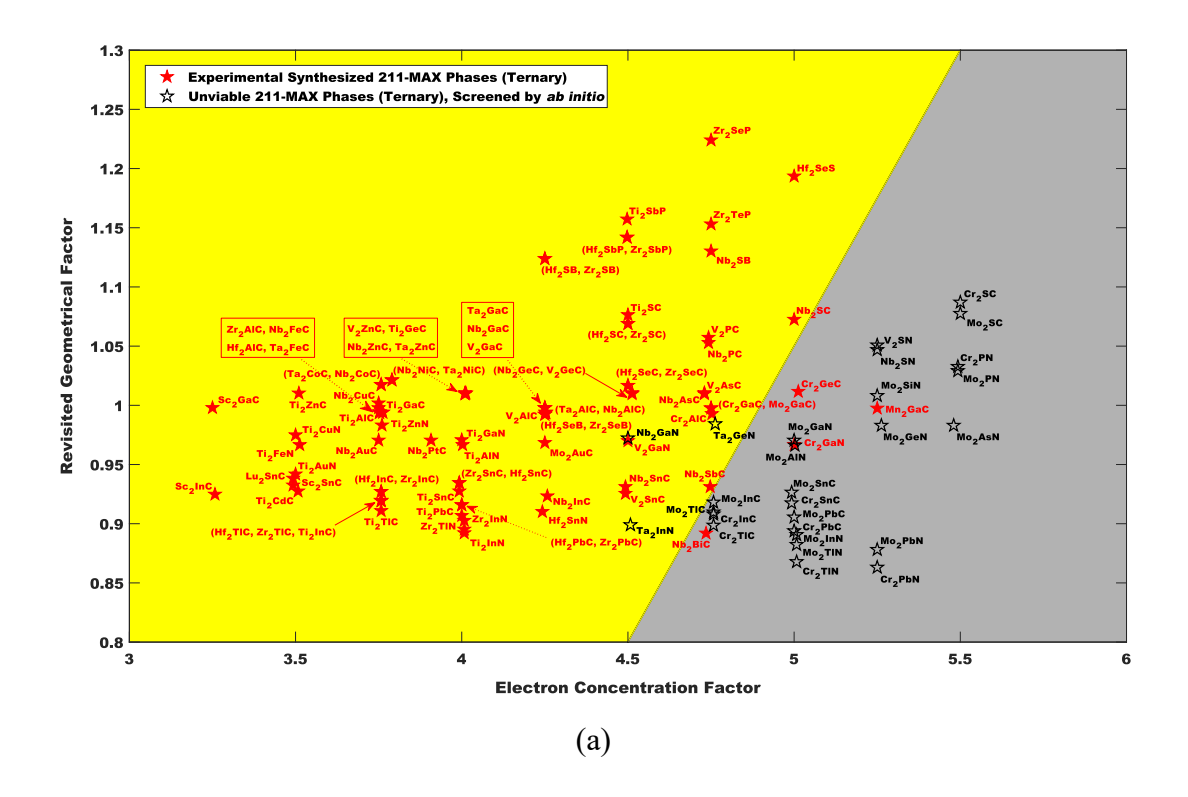
- intermetallic compounds, J. Less-Common Met. 92 (1983) 215-238.
- [52] P. Villars, K. Brandenburg, M. Berndt, S. LeClair, A. Jackson, Y.H. Pao, B. Igelnik, M. Oxley, B. Bakshi, P. Chen, S. Iwata, Binary, ternary and quaternary compound former/nonformer prediction via Mendeleev number, J. Alloys Compd. 317 (2001) 26-38.
- [53] Z. Allahyari, A.R. Oganov, Nonempirical definition of the Mendeleev numbers: organizing the chemical Space, J. Phys. Chem. C 124 (2020) 23867-23878.
- [54] P.M. Clark, S. Lee, D.C. Fredrickson, Transition metal AB<sub>3</sub> intermetallics: Structure maps based on quantum mechanical stability, J. Solid State Chem. 178 (2005) 1269-1283.
- [55] J. Hauck, W. Erkens, K. Mika, K. Wincerath, Structure maps for polymer structures, Int. J. Mod. Phys. B 16 (2002) 3449-3457.
- [56] J. Hauck, K. Mika, Structure maps for crystal engineering, Cryst. Eng. 5 (2002) 105-121.
- [57] A.S. Korotkov, N.M. Alexandrov, Structure quantitative map in application for AB<sub>2</sub>X<sub>4</sub> system, Comput. Mater. Sci. 35 (2006) 442-446.
- [58] H. Zhang, N. Li, K. Li, D. Xue, Structural stability and formability of ABO<sub>3</sub>-type perovskite compounds, Acta Crystallogr., Sect. B: Struct. Sci 63 (2007) 812-818.
- [59] K. Rajan, Chapter 15 Informatics for crystallography: designing structure maps, in:K. Rajan (Ed.), Informatics for Materials Science and Engineering, Butterworth-Heinemann, Oxford, 2013, pp. 365-383.
- [60] W.-Y. Ching, Materials informatics using ab initio data: application to MAX phases, in: T. Lookman, F.J. Alexander, K. Rajan (Eds.), Information Science for Materials Discovery and Design, Springer International Publishing, Cham, 2016, pp. 187-212.
- [61] W.M. Haynes, D.R. Lide, T.J. Bruno, CRC Handbook of Chemistry and Physics: A

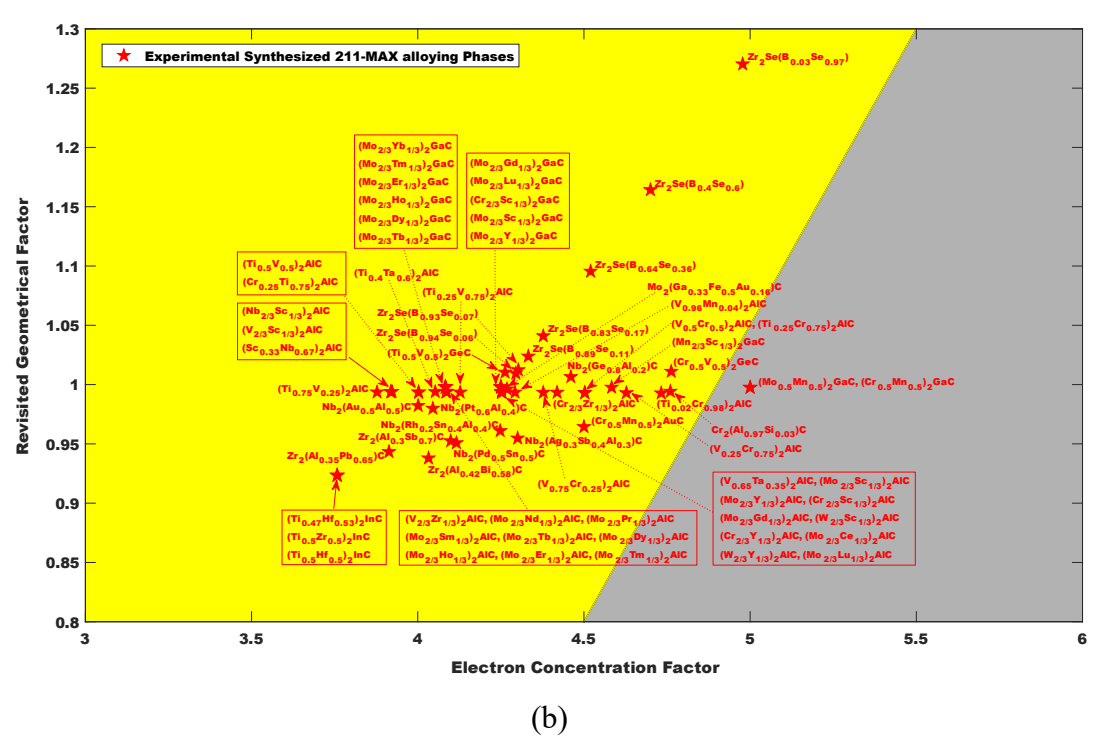
- Ready-reference Book of Chemical and Physical Data, 96<sup>th</sup> edition. ed., CRC Press, 2016. pp. 9-49, 9-50
- [62] U. Mizutani, Hume-Rothery Rules for Structurally Complex Alloy Phases, CRC Press, Boca Raton, FL, 2011.
- [63] U. Mizutani, H. Sato, The physics of the Hume-Rothery electron concentration rule, Crystals 7 (2017) 9.
- [64] U. Mizutani, H. Sato, Determination of electrons per atom ratio for transition metal compounds studied by FLAPW-Fourier calculations, Philos. Mag. 96 (2016) 3075-3096.
- [65] U. Mizutani, H. Sato, T.B. Massalski, The original concepts of the Hume-Rothery rule extended to alloys and compounds whose bonding is metallic, ionic, or covalent, or a changing mixture of these, Prog. Mater Sci. 120 (2021) 100719.
- [66] M. Weller, T. Overton, J. Rourke, F. Armstrong, Inorganic Chemistry, 7<sup>th</sup> edition, Oxford University Press, 2018.
- [67] L.E. Toth, Transition Metal Carbides and Nitrides, Academic Press, New York; London, 1971.
- [68] W. Hume-Rothery, Factors affecting the stability of metallic phases, in: P.S. Rudman, J. Stringer, R.I. Jaffee (Eds.), Phase Stability in Metals and Alloys, McGraw-Hill, New York, 1967, pp. 3-23.
- [69] W. Hume-Rothery, G.W. Mabbott, K.M.C. Evans, The freezing points, melting points, and solid solubility limits of the alloys of silver and copper with the elements of the B sub-groups, Phil. Trans. R. Soc. A 233 (1934) 1-97.
- [70] Y.M. Zhang, S. Yang, J.R.G. Evans, Revisiting hume-rothery's rules with artificial neural networks, Acta Mater. 56 (2008) 1094-1105.
- [71] C.J. Bartel, C. Sutton, B.R. Goldsmith, R. Ouyang, C.B. Musgrave, L.M.

- Ghiringhelli, M. Scheffler, New tolerance factor to predict the stability of perovskite oxides and halides, Sci. Adv. 5 (2019) eaav0693.
- [72] M.R. Filip, F. Giustino, The geometric blueprint of perovskites, PNAS 115 (2018) 5397-5402.
- [73] C. Li, X. Lu, W. Ding, L. Feng, Y. Gao, Z. Guo, Formability of ABX<sub>3</sub> (X = F, Cl, Br, I) halide perovskites, Acta Crystallogr., Sect. B: Struct. Sci. 64 (2008) 702-707.
- [74] C. Li, K.C.K. Soh, P. Wu, Formability of ABO<sub>3</sub> perovskites, J. Alloys Compd. 372 (2004) 40-48.
- [75] S.D. Cotton, Lanthanide and Actinide Chemistry, John Wiley, Chichester, 2006.
- [76] H. Ding, Y. Li, J. Lu, K. Luo, K. Chen, M. Li, P.O.A. Persson, L. Hultman, P. Eklund, S. Du, Z. Huang, Z. Chai, H. Wang, P. Huang, Q. Huang, Synthesis of MAX phases Nb<sub>2</sub>CuC and Ti<sub>2</sub>(Al<sub>0.1</sub>Cu<sub>0.9</sub>)N by A-site replacement reaction in molten salts, Mater. Res. Lett. 7 (2019) 510-516.
- [77] M. Li, J. Lu, K. Luo, Y. Li, K. Chang, K. Chen, J. Zhou, J. Rosen, L. Hultman, P. Eklund, P.O.A. Persson, S. Du, Z. Chai, Z. Huang, Q. Huang, Element replacement approach by reaction with lewis acidic molten salts to synthesize nanolaminated max phases and mxenes, J. Am. Chem. Soc. 141 (2019) 4730-4737.
- [78] X. He, Y. Bai, C. Zhu, Y. Sun, M. Li, M.W. Barsoum, General trends in the structural, electronic and elastic properties of the M<sub>3</sub>AlC<sub>2</sub> phases (M=transition metal): A first-principle study, Comput. Mater. Sci. 49 (2010) 691-698.
- [79] Z. Liu, E. Wu, J. Wang, Y. Qian, H. Xiang, X. Li, Q. Jin, G. Sun, X. Chen, J. Wang, M. Li, Crystal structure and formation mechanism of (Cr<sub>2/3</sub>Ti<sub>1/3</sub>)<sub>3</sub>AlC<sub>2</sub> MAX phase, Acta Mater. 73 (2014) 186-193.
- [80] E.N. Caspi, P. Chartier, F. Porcher, F. Damay, T. Cabioc'h, Ordering of (Cr,V) Layers in Nanolamellar (Cr<sub>0.5</sub>V<sub>0.5</sub>)<sub>n+1</sub>AlC<sub>n</sub> Compounds, Mater. Res. Lett. 3 (2015) 100-106.

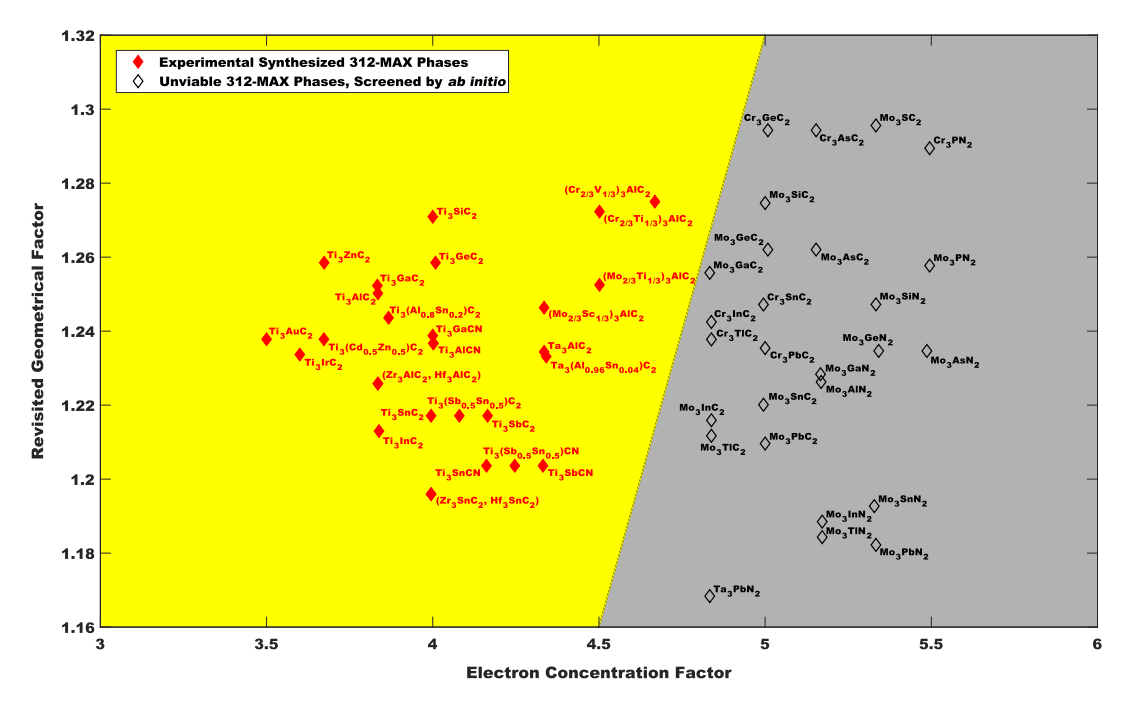
- [81] R. Meshkian, Q. Tao, M. Dahlqvist, J. Lu, L. Hultman, J. Rosen, Theoretical stability and materials synthesis of a chemically ordered MAX phase, Mo<sub>2</sub>ScAlC<sub>2</sub>, and its two-dimensional derivate Mo<sub>2</sub>ScC<sub>2</sub> MXene, Acta Mater. 125 (2017) 476-480.
- [82] B. Anasori, M. Dahlqvist, J. Halim, E.J. Moon, J. Lu, B.C. Hosler, E.a.N. Caspi, S.J. May, L. Hultman, P. Eklund, J. Rosen, M.W. Barsoum, Experimental and theoretical characterization of ordered MAX phases Mo<sub>2</sub>TiAlC<sub>2</sub> and Mo<sub>2</sub>Ti<sub>2</sub>AlC<sub>3</sub>, J. Appl. Phys. 118 (2015) 094304.
- [83] O. Muller, R. Roy, The Major Ternary Structural Families, Springer, Berlin; New York, 1974.
- [84] H.D. Megaw, J. Barber, Crystal Structures: A Working Approach, Saunders, Philadelphia; London, 1973.
- [85] R.D. Shannon, Revised effective ionic radii and systematic studies of interatomic distances in halides and chalcogenides, Acta Cryst. 32 (1976) 751-767.
- [86] V.M. Goldschmidt, Die Gesetze der Krystallochemie, Naturwissenschaften 14 (1926) 477-485.
- [87] L. Pauling, Nature of the Chemical Bond, 3<sup>rd</sup> Edition. Cornell University Press, 1960.
- [88] Q.Z. Tao, M. Dahlqvist, J. Lu, S. Kota, R. Meshkian, J. Halim, J. Palisaitis, L. Hultman, M.W. Barsoum, P.O.A. Persson, J. Rosen, Two-dimensional Mo<sub>1.33</sub>C MXene with divacancy ordering prepared from parent 3D laminate with in-plane chemical ordering, Nat. Commun. 8 (2017) 14949.
- [89] M. Dahlqvist, J. Lu, R. Meshkian, Q.Z. Tao, L. Hultman, J. Rosen, Prediction and synthesis of a family of atomic laminate phases with Kagome-like and in-plane chemical ordering, Sci. Adv. 3 (2017) e1700642.
- [90] B. Manoun, S.K. Saxena, G. Hug, A. Ganguly, E.N. Hoffman, M.W. Barsoum, Synthesis and compressibility of Ti<sub>3</sub>(Al,Sn<sub>0.2</sub>)C<sub>2</sub> and Ti<sub>3</sub>Al(C<sub>0.5</sub>,N<sub>0.5</sub>)<sub>2</sub>, J. Appl. Phys.

- 101 (2007) 113523.
- [91] T. Cabioch, P. Eklund, V. Mauchamp, M. Jaouen, M.W. Barsoum, Tailoring of the thermal expansion of Cr<sub>2</sub>(Al<sub>x</sub>,Ge<sub>1-x</sub>)C phases, J. Eur. Ceram. Soc. 33 (2013) 897-904.
- [92] T. Lapauw, B. Tunca, D. Potashnikov, A. Pesach, O. Ozeri, J. Vleugels, K. Lambrinou, The double solid solution (Zr, Nb)<sub>2</sub>(Al, Sn)C MAX phase: a steric stability approach, Sci. Rep. 8 (2018) 12801.
- [93] H. Fashandi, M. Dahlqvist, J. Lu, J. Palisaitis, S.I. Simak, I.A. Abrikosov, J. Rosen, L. Hultman, M. Andersson, A.L. Spetz, P. Eklund, Synthesis of Ti<sub>3</sub>AuC<sub>2</sub>, Ti<sub>3</sub>Au<sub>2</sub>C<sub>2</sub> and Ti<sub>3</sub>IrC<sub>2</sub> by noble metal substitution reaction in Ti<sub>3</sub>SiC<sub>2</sub> for high-temperature-stable Ohmic contacts to SiC, Nat. Mater. 16 (2017) 814-818.
- [94] M. Nechiche, T. Cabioc'h, E.N. Casp, O. Rivin, A. Hoser, V. Gauthier-Brunet, P. Chartier, S. Dubois, Evidence for symmetry reduction in Ti<sub>3</sub>(Al<sub>1-δ</sub>Cu<sub>δ</sub>)C<sub>2</sub> MAX phase solid solutions, Inorg. Chem. 56 (2017) 14388-14395.
- [95] M. Nechiche, V. Gauthier-Brunet, V. Mauchamp, A. Joulain, T. Cabioc'h, X. Milhet,
   P. Chartier, S. Dubois, Synthesis and characterization of a new (Ti<sub>1-ε</sub>,Cu<sub>ε</sub>)<sub>3</sub>(Al,Cu)C<sub>2</sub>
   MAX phase solid solution, J. Eur. Ceram. Soc. 37 (2017) 459-466.
- [96] B. Gou, L. Wang, B. Ye, C. Meng, X. Li, Q. Chen, T. Yang, W. Xu, Low-temperature synthesis of pure-phase Ti<sub>3</sub>(Al, Fe)C<sub>2</sub> solid solution with magnetic monoatomic layers by replacement reaction, J. Mater. Sci.: Mater. Electron. 32 (2021) 13081-13088.

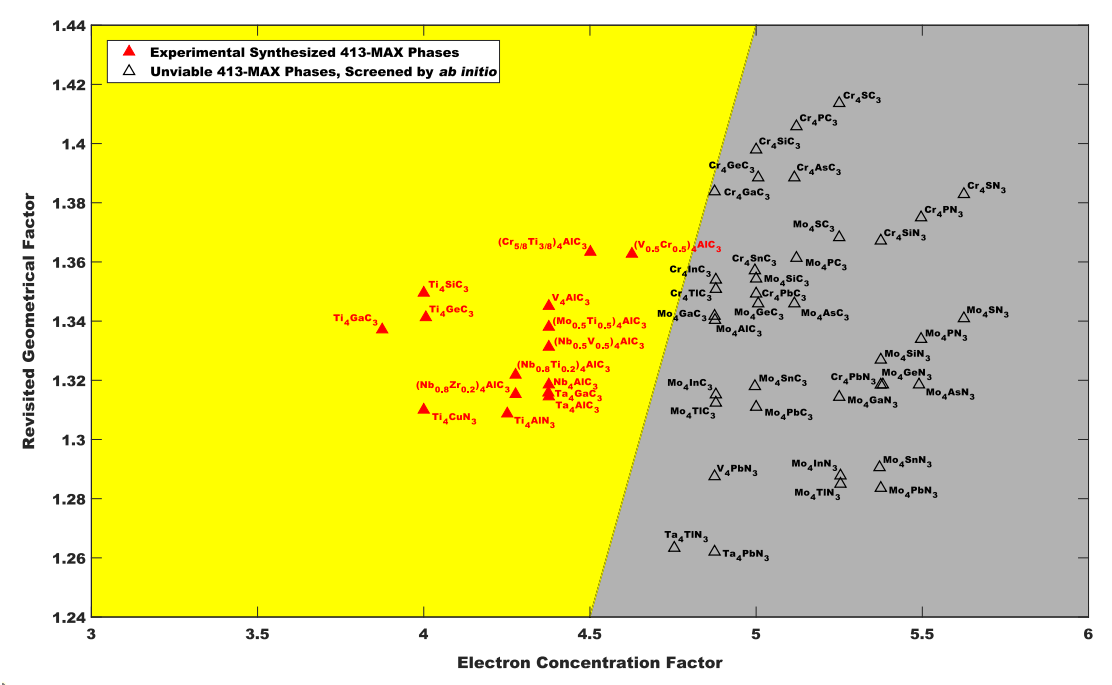




S1 The structure maps constructed *via* revisited geometrical and electron concentration factors for (a) 211-MAX phases (ternary) and (b) 211-MAX alloying phases (with full set of labels).



S2 The structure maps constructed *via* revisited geometrical and electron concentration factors for 312-MAX phases (with full set of labels).



S3 The structure maps constructed *via* revisited geometrical and electron concentration factors for 413-MAX phases (with full set of labels).